1	Eco-hydrological responses to recent droughts in tropical South America
2	Yelin Jiang ^a , Meijian Yang ^a , Weiguang Liu ^a , Koushan Mohammadi ^a , Guiling Wang ^{a,b} *
3	^a Department of Civil and Environmental Engineering, University of Connecticut, Storrs, CT
4	USA
5	^b Center for Environmental Sciences and Engineering, University of Connecticut, Storrs, CT
6	USA
7	* Correspondence: guiling.wang@uconn.edu; 860 486 5648
8	
9	
10	
11	
12	
13	
	Sylvanitted to Empiremental Desegrable Lettons
14	Submitted to Environmental Research Letters
15	June 9, 2021 (initial submission)
16	August 9, 2021 (revised)
17	September 25, 2021 (second revision)
18	

Abstract

19

20 This study assesses the ecohydrological effects of recent meteorological droughts in tropical South 21 America based on multiple sources of data, and investigates the possible mechanisms underlying 22 the drought response and recovery of different ecohydrological systems. Soil drought response and 23 recovery lag behind the meteorological drought, with delays longer in the dry region (Nordeste) 24 than in the wet region (Amazonia), and longer in deep soil than in shallow soil. ET and vegetation 25 in Nordeste are limited by water under normal conditions and decrease promptly in response to 26 the onset of shallow soil drought. In most of the Amazon where water is normally abundant, ET 27 and vegetation indices follow an increase-then-decrease pattern, increase at the drought onset due 28 to increased sunshine and decrease when the drought is severe enough to cause a shift from an 29 energy-limited regime to a water-limited regime. After the demise of meteorological droughts, ET 30 and vegetation rapidly recover in Nordeste with the replenishment of shallow soil moisture, but 31 take longer to recover in southern Amazon due to their dependence on deep soil moisture storage. 32 Following severe droughts, the negative anomalies of ET and vegetation indices in southern 33 Amazon tend to persist well beyond the end of soil drought, indicating drought-induced forest 34 mortality that is slow to recover from. Findings from this study may have implications on the 35 possibility of a future forest dieback as drought is projected to become more frequent and more 36 severe in a warmer climate.

- 37 Keywords: Drought; Land-atmosphere interactions; Soil moisture; ET; Vegetation responses;
- 38 tropical South America

1. Introduction

40

41

42

43

44

45

46

47

48

49

50

51

52

53

54

55

56

57

58

59

60

61

62

63

64

65

66

67

68

69

Drought is a major natural hazard characterized by below-normal precipitation over a period of months to years, which has devastating impacts on agriculture, water resources, and the economy (Dai 2011, Sheffield et al 2012, Smith and Matthews 2015). Globally, drought is projected to increase in frequency and severity, mainly as a result of decreasing rainfall and increasing evaporation in a warmer climate (Wang 2005, Sheffield and Wood 2008b, Dai 2013, Su et al 2018, Naumann et al 2018). Observational data have already shown an increasing trend of drought frequency and severity, despite the debates on the magnitude of changes (Trenberth et al 2014, Sheffield et al 2012, Dai 2013). At the regional scale, as a critical component of the global ecosystem, tropical South America has experienced repeated severe and widespread droughts over the past two decades. El Niño-Southern Oscillation (ENSO) and warm anomalies in the tropical North Atlantic are two main drivers of meteorological droughts over tropical South America (Zeng et al 2008, Coelho et al 2012, Panisset et al 2018, Jimenez et al 2018). In the Amazon rainforest, extreme droughts in 2005, 2010 and 2016 were all considered one-in-100-year events, contributing to an increasing trend of drought severity and spatial extent during the past 20 years (Jiménez-Muñoz et al 2016). The Nordeste region also experienced two major droughts in 2007 and 2012 (Marengo et al., 2017); the extreme drought in 2012 reached the strongest intensity in 2012/2013 but lasted until 2015 at a somewhat lower intensity. The prolonged 2012 drought was followed by the unprecedented drought in 2016 to produce severe and long-lasting water deficits in Northeast Brazil (Erfanian et al 2017), putting the regional ecosystem at risk.

Soil moisture is an important pathway for precipitation anomalies to influence the regional ecosystem. Low soil moisture inhibits latent heat flux and thus enhances sensible heat flux, leading to warmer air in the lower atmosphere (Seneviratne *et al* 2010, Stocker *et al* 2019, Wang *et al* 2007, Liu *et al* 2014). In turn, higher temperature increases the vapor pressure deficit and evaporative demand, which may accelerate evapotranspiration and further deplete soil moisture (Ruosteenoja *et al* 2018). Moreover, soil water availability directly modulates vegetation activities. Soil moisture depletion breaks down the soil-plant-atmosphere hydraulic gradient that drives the water transport for transpiration, leading to plant water stress and reduction of vegetation productivity (Rodriguez-Iturbe 2000). However, the response of soil

moisture lags precipitation anomalies by days to months (Koster and Suarez 2001, Koster *et al* 2010, Liu *et al* 2014, Kim and Wang 2007a, 2007b), as soil acts as a temporary reservoir to accumulate precipitation anomalies and retain the impact of antecedent conditions. For example, negative anomalies of soil water storage resulting from a meteorological drought may take a long time to be replenished even by above-normal rainfall. Similarly, it takes time for evapotranspiration to deplete the above-normal soil moisture following a period of abundant rain. This "carryover" effect of soil moisture, also known as soil moisture memory, depends on the local hydroclimate regime (Rahman *et al* 2015), and is therefore expected to vary substantially between the humid and dry regions of the tropical South America.

70

71

72

73

74

75

76

77

78

79

80

81

82

83

84

85

86

87

88

89

90

91

92

93

94

95

96

97

98

99

Due to the sparsity of the field stations in Amazonia, monitoring the ecological responses to droughts is challenging. Some previous studies based on satellite data found a greening-up signal in the Amazon rainforest during dry years or dry seasons (Huete et al 2006, Saleska et al 2016, 2007), while others found an opposite signal based on the same source of data but different data filtering methods (Samanta et al 2010, 2011, Xu et al 2011). A major cause for such uncertainties has to do with cloud and aerosol contamination leaving a very low number of clear sky observations. This debate is also a reflection of the uncertainty regarding whether the Amazon hydroclimate regime at the beginning of the dry season is energy-limited or waterlimited. More recently, Amazon region has been increasingly considered as an energy-limited regime where increased solar radiation during droughts may temporarily increase vegetation productivity (Guan et al 2015, Yang et al 2018, Jiang et al 2020). However, a severe or longlasting drought would ultimately deplete the soil moisture storage and cause water stress on vegetation. In addition, differences among vegetation properties described by different indices add to the uncertainties. Nearly half of the global vegetated areas have experienced inconsistent trends in vegetation cover, greenness and productivity, and this is especially puzzling in tropical broadleaf evergreen forests where vegetation greenness and productivity often show opposite trends (Ding et al 2020). Moreover, Yang et al. (2018) found that forest greenness and photosynthesis in Amazon are largely decoupled during the drought in 2016, indicating that the vegetation photosynthetic capacity may have been suppressed despite the slight increase in greenness.

The ecohydrological responses to individual droughts in the Amazon forest have been

widely studied, yet no clear consensus has emerged. Much less studied and less understood is how different ecosystems in tropical South America may differ in responding to the sometimes recurrent droughts. This research gap hampers the development of predictive understanding of the fate of the terrestrial ecosystems in a warmer world with more severe and frequent extreme events. Here, based on multiple sources of data and model estimation, we investigate how the hydrological cycle and vegetation in different sub-regions of the tropical South America responded to droughts in the past two decades, and explore the possible physical mechanisms that influence the ecohydrological recovery from droughts.

2. Data and Methodology

100

101

102

103

104

105

106

107

108

109

110

111

112

113

114

115

116

117

118

119

120

121

122

123

124

125

126

127

128

To quantify the ecohydrological responses in different parts of the tropical South America, we select three sub-regions based on vegetation coverages and rainfall regimes (Figure 1). The Amazon basin is covered predominantly by tropical evergreen forest, but the northern part is substantially wetter than the southern part. Here we use 5°S as the boundary to divide the basin into the southern Amazon (73°W-50°W, 15°S-5°S) and northern Amazon (73°W-50°W, 5°S-5°N). The Nordeste region (50°W-34°W, 20°S-5°S) in Northeast Brazil, consisting primarily of cropland and grassland with dispersed drought deciduous forest, is identified as one of the world's most vulnerable regimes to climate change (IPCC 2014). It's also the world's most densely populated semiarid region, with a population density of 34 people/km² in 2010 (Marengo et al 2017). Wet season in the Amazon is defined as the period when daily precipitation exceeds 6.1 mm/day, following the method of Li and Fu (2004); dry season is defined as the period with daily precipitation less than 3 mm/day. The northern Amazon is rainy throughout the year, with an eight-month wet season (December-to-July) and no dry season (Figure 1e). The southern Amazon has a strong rainfall seasonality, with a wet season from November to April and a dry season from June to September. In Nordeste, precipitation climatology shows a clear seasonality with more than 4 mm/day of rain during November-March and less than 2 mm/day of rain during May-September. We therefore refer to these two periods as Nordeste's wet season and dry season respectively. The ecohydrological responses to droughts and the underlying physical mechanisms in the three sub-regions may differ due to differences in vegetation and hydroclimatic conditions.

To account for the data-related uncertainties, we use monthly data from multiple sources, including gauge-based data (GPCC, CRU), satellite observations (TRMM, GRACE, MODIS, GOME-2, FLASHFlux), reanalysis data (ERA5), and model simulations (GLEAM, GLDAS). These data differ in spatial resolution, temporal resolution, and the data record length used as reference for estimating statistical parameters (Table 1), and data for a given variable from different sources often differ even in climatology. To minimize the impact of differences in climatology among different data sources, most of our analyses were based on standardized anomalies. For a given monthly time series from each data source, the standardized anomalies were derived by removing the long-term mean for each of the twelve months and dividing the anomalies by the standard deviation the corresponding month. Based on availability of most of the datasets used, we choose 2000-2018 as our study period.

Both GLDAS and ERA5 include soil moisture (SM) data in multiple layers at different depths. SM response to meteorological droughts depends on the soil depth, and its impact on vegetation functioning also depends on the root depth. Most (~85%) roots of grass and crops are in the top 0.5m of the soil, while tree roots can reach a depth of up to several meters (United States Department of Agriculture and Service 2005, Zeng 2001). In this study, our analysis of SM is conducted at two general depths: shallow soil and deep soil. We chose the layer of 0-28cm in ERA5 and 0-40cm in GLDAS as the representative shallow soil; used as the representative deep soil is the layer of 100-289cm in ERA5 and 100-200cm in GLDAS, the deepest layer available in each product. In addition to SM at different depths, GRACE territorial water storage (TWS) data provides information on total water storage including both SM and groundwater.

Remote sensing data for vegetation in the Amazon, including MODIS (on gross primary productivity (GPP), ET, and normalized difference vegetation index (NDVI)) and GOME-2 (solar-induced chlorophyll fluorescence (SIF)) data, is heavily affected by the presence of clouds and biomass burning aerosols. For each grid cell, there is only a limited number of clear sky observations within a month. This data limitation is a major cause for uncertainties in past studies on whether vegetation greens up or not during drought events (Hashimoto *et al* 2021). To alleviate the data paucity, we aggregate the data spatially and conduct most of the analysis based on averages over each sub-region. Specifically, we averaged the raw data across all grid cells within a sub-region first; the resulting monthly time series were then processed to derive the

standardized anomalies time series.

A sub-region is considered to be in a dry event when majority of the precipitation products (at least three out of four) show a negative anomaly. Sheffield & Wood (2008a) suggested to characterize droughts using intensity and duration, and the multiplicative effect of the two can be considered a severity metric. Here, we define three categories of meteorological droughts considering both duration and intensity thresholds. A mild drought is defined as a dry event longer than three months with the intensity (standardized anomaly) reaching -0.5 for at least one month; a severe drought is defined as a dry event longer than six months with the intensity reaching -0.75 for at least two months; an extreme drought is defined as a dry event longer than twelve months with the intensity reaching -1.0 for at least four months. These chosen duration and intensity thresholds are meant to identify events with ecohydrological and socioeconomic impacts at the seasonal to inter-annual time scales. In our analysis, we focus on ecohydrological responses to major droughts in tropical South America, including droughts of 2005, 2007, 2010, 2012, and repeated droughts during 2015-2018, and define the recovery period of the ecohydrological system as the period from the demise of meteorological drought to the time when the standardized anomalies of the ecohydrological variables first return to zero.

3. Results

The standardized anomalies of precipitation estimated based on different products are used to characterize meteorological droughts. Figure 2 presents the time series of standardized anomalies of spatially averaged precipitation over the Nordeste region, southern and northern Amazon from ERA5, TRMM, GPCC, and CRU. Note that for each sub-region, precipitation from different datasets during 2001-2018 exhibit consistent inter-annual variation and suggest similar drought characteristics. This is not without exception. For example, over Amazonia, the CRU gauge-based data diverges from the other three products, likely due to the gridding of sparse station data through interpolation. Rainfall estimation over Amazonia is subject to large uncertainties due to the lack of sufficient in-situ observations in hard-to-access forest regions, especially in northern Amazon and during early years of the study period (Wang and Dickinson 2012). To account for this data uncertainty, here we define a meteorological drought when the precipitation standardized anomalies meet the drought criteria in at least three of the four datasets.

Based on the precipitation time series in Figure 2, meteorological droughts of all three categories were identified for each sub-region; their durations are marked by the color shading in Figure 2 (and in other plots of ecohydrological time series), and the corresponding start and end time are shown in Table 2. Our result analyses focus on ecohydrological responses to and recovery from these meteorological droughts.

3.1 Soil moisture responses

SM is the link between meteorological drought and ecosystem responses, as SM directly influences plant water availability and limits photosynthesis and productivity. Both evapotranspiration depleting the SM storage and moisture transport within the soil are slow processes, leading to a relatively long time scale for SM variability ranging from weeks to months or longer (Liu *et al* 2014). As a result of this SM carryover effect, soil drought lags meteorological drought, leading to lagged ecosystem responses. Ecological responses to soil drought are dominated by water availability in the root zone, the depth of which varies with vegetation type. Tree roots in the Amazon region are abundant in both shallow and deep soils, with tap roots reaching as deep as 18 m (Nepstad *et al* 1994); in Nordeste, land cover is dominated by grass and crops (Figure 1), with most of the roots in shallow soil. Overall, the SM temporal variations from ERA5 and GLDAS in Figure 3 show a high degree of consistency, despite the slight differences in the thickness and depth of soil layers chosen to represent shallow or deep soil.

In Nordeste, the carryover effect of SM is strong (Figure 3a). Under wet initial conditions, a mild meteorological drought may not translate to soil drought. For example, due to the slow dissipation of the wet soil anomalies carried over from the previous year, no soil drought was detected in Nordeste during the mild droughts in 2005 and 2010. For severe meteorological droughts, soil drought would ultimately occur, with longer onset delays in deeper soil than in shallow soil, due to the slow transport of moisture within the soil and the smaller fraction of plant roots (therefore water uptake) in deeper soil. The onset of deep soil drought was seven months later than the severe meteorological drought of 2007 in ERA5 (November 2007), but was rapid without much delay in GLDAS, indicating a large degree of uncertainties in different SM products. The deep soil reached its peak drought intensity in the last month of the 2007 meteorological drought, and fully recovered with a delay of just one month due to replenishment

by rainfall in the wet season (February 2008). However, the recovery process is very different following the 2012 severe meteorological drought, one of the most extreme droughts in Nordeste. Although the shallow soil storage got replenished within seven months after the 2012 drought (May 2013), the deep layer soil storage stayed depleted and showed little sign of recovery by the time of the 2016 extreme drought (Figure 4). The deep soil drought therefore extended to 2018 without a break, leading to an extreme long-term soil drought and a continuous desiccation trend (Figure 4). Consistent with the deep SM response, the GRACE TWS (albeit intermittent due to several months of missing data) also did not recover from the 2012 drought in Nordeste (Figure 3a). In contrast, shallow SM reached full recovery during the breaks between the repeated droughts during 2015-2018.

218

219

220

221

222

223

224

225

226

227

228

229

230

231

232

233

234

235

236

237

238

239

240

241

242

243

244

245

246

247

248

Unlike the semiarid climate in Nordeste, the southern Amazon is generally humid, and soil during the wet season is often saturated, showing little year-to-year variation. Due to the small magnitude of inter-annual variability, a small reduction in SM can be translated to a large magnitude of standardized anomaly. It is easier for SM in the southern Amazon to fully recover after the demise of the meteorological drought, due primarily to the typically large amount of wet-season rainfall that can quickly replenish the soil storage. Due to the seasonality of precipitation in the southern Amazon, the SM responses and recovery depend heavily on the drought occurrence time, with typically faster onset and recovery during the wet season than dry season (Figure 3b). For example, the mild meteorological drought in 2007 started in the wet season (February 2007) when the SM level is typically high and standard deviation low, leading to a quick growth of standardized anomalies and rapid onset of soil drought; the meteorological drought ended during the dry season in September 2007, but SM did not fully recover until several months later (December 2007 in GLDAS or January 2008 in ERA5). Similarly, the onset of soil drought in 2012 lagged the mild meteorological drought only slightly. The SM recovery from the 2012 drought is earlier in ERA5 than in GLDAS, but both closely follow the demise of the meteorological drought in a wet season in the corresponding dataset (November 2012 in ERA5 and two months later in the other three datasets). The severe meteorological drought in 2005 and 2010 both started in the wet season and ended right before the wet season, with short delays in the soil drought response for both onset and recovery (0-2 months). In contrast, the extreme meteorological drought in 2016 started with a relative dry soil condition during the dry season (August 2015) when standard deviation is large, leading to a relatively long lag of several

months for the deep soil drought response. Although the intensity of 2016 meteorological drought in southern Amazon is the strongest among the three sub-regions (Figure 2), the SM in southern Amazon can quickly recover to the normal level in wet seasons during the break between the repeated droughts during 2015-2018 (Figure 3b).

249

250

251

252

253

254

255

256

257

258

259

260

261

262

263

264

265

266

267

268

269

270

271

272

273

274

275

276

277

In the wet climate of northern Amazon, the lag in soil drought response including both the onset and recovery is even weaker (Figure 3c), due to the small magnitude of inter-annual variability and the larger amount of wet season precipitation. As such, the mild meteorological droughts in 2005 and 2007 had limited impacts on SM, as soil stays at a fairly high saturation level during the short periods of negative precipitation anomalies. The 2012 drought in northern Amazon was divided into two segments by a brief rainfall recovery in August, but the soil drought continued, as one month of normal rainfall was not sufficient to replenish the depleted soil water storage. The soil drought in 2012 lagged the meteorological drought by one month at onset due to the wet initial condition, and by a longer period at recovery that differ between ERA5 (with no delay in shallow layer and three months delay in deeper layer) and GLDAS (with five months delay in both layers). This discrepancy between ERA5 and GLDAS reflects the large uncertainties in SM estimation. Contrary to the Nordeste region, the Amazon basin hydrologically recovered to normal levels soon after the 2012 drought. Before the onset of both the severe meteorological drought in 2010 and the extreme meteorological drought in 2016, northern Amazon had already experienced lower-than-normal precipitation for several months (although not reaching the threshold for our drought definition). For this reason, in both cases the soil drought onset did not lag the meteorological drought. Similar to other regions, soil drought recovery tends to be rapid when the meteorological drought demise occurs during a relatively wet time of the year, as was the case for both the 2010 drought (ending in April 2010) and the 2016 drought (ending in August 2016); deeper soil water storage took longer (1-4 months depending on the data source) to replenish. For the 2017 meteorological drought, its demise occurs in a relative dry season (September 2017), which caused longer delays in SM recovery than during the 2016 drought. Note that due to the humid climate in this sub-region, even though the SM standardized anomalies indicate a drought, the actual level of soil saturation may still be quite high.

3.2 Evaporative responses

As an important component of the terrestrial hydrological cycle, evapotranspiration (ET) is closely coupled with SM dynamics, plant photosynthesis, and the surface energy cycle (Jung et al 2010). ET increases approximately linearly with SM to a certain threshold (approximately 0.4 m³/m³ in the study domain), and then plateaus or even decreases (Figure 5). This threshold marks the transition from a water-limited ET regime to an energy-limited regime. The decrease, if present, reflects a decrease of energy availability caused by increased cloudiness during precipitation events in wet regions/seasons with no water limitation on ET. Humid regions may transition from an energy-limited regime to a water-limited regime during dry seasons or during drought events (Figures 5b and 5c).

During droughts, in addition to the direct effect of SM limiting root water update (therefore transpiration), vapor pressure deficit (VPD) is also an important influencing factor (Zhou *et al* 2019). VPD results from lack of moisture and/or high temperature, both of which are common during drought events. Since VPD reflects the atmospheric evaporative demand, ET increases with VPD under mild conditions; however, when VPD reaches a certain threshold (~0.6 kPa in the study domain), plant physiological response (to heat and/or drought) kicks in with a partial closure of leaf stomata, which reduces transpiration (Katul *et al* 2009). Low SM and high VPD typically co-occur (Koster *et al* 2010, De Boeck and Verbeeck 2011, Zhou *et al* 2019), so the SM limitation and high VPD may have multiplicative effects on ET. These physical and physiological relationships underlie the ET patterns shown in Figure 5.

Figure 6 demonstrates how ET responded to different droughts in tropical South America based on ERA5, MODIS, GLEAM and GLDAS. Different ET products generally feature similar temporal variability in Nordeste but demonstrate larger uncertainties in the Amazon basin where the GLDAS ET clearly diverges from the other three products. In Nordeste, climate is semiarid and vegetation cover is primarily grass or crops with a shallow root system, so water availability can be a limiting factor for ET. Indeed, the ET variation (Figure 6a) closely resembles the shallow SM variation (Figure 3a) with a highly linear correspondence (Figure 5a), indicating that ET is strongly constrained by shallow SM. On the contrary, deep SM has a greater impact on ET in the Amazon region as trees have longer roots tapping moisture in deeper soil.

In Nordeste, the mild meteorological drought in 2005 and 2010 did not lead to soil

drought and therefore have little impact on ET (Figure 6a). During the severe meteorological drought in 2007 and 2012, ET responses are all rapid at the onset stage; consistent with the shallow SM signals, the ET recovery from drought takes longer, lagging the demise of the meteorological drought by eight months for the 2012 drought (with ET recovery in June 2013) and one month for the 2007 drought (with ET recovery in March 2008). In the middle of the 2016 extreme drought during the rainy season, despite the below normal precipitation and SM, it appears that water availability is still sufficient to sustain a relatively high level of ET. Indeed, as shown in Figure 7e3, the soil saturation level is approximately 60%~80% in Nordeste during the corresponding season.

Estimating ET in the Amazon basin is challenging, due to thick clouds complicating satellite remote sensing, limited number of flux towers, and diversity of models and model inputs (Sörensson and Ruscica 2018, Badgley *et al* 2015, Wu *et al* 2020). During droughts in the Amazon, our results show that ET generally tends to increase first and then decrease (Figures 6b and 6c). At the onset or early stage of the drought, the decrease in cloudiness allows more solar radiation to reach the ground, increasing energy availability and surface temperature (Figures 8b and 8c) therefore VPD, which accelerates ET. As the drought progresses, SM is depleted and temperature as well as VPD further increases. These ultimately cause ET to decrease and to shift from an energy-limited regime to a water-limited regime (Figure 5). Plant in southern Amazon would eventually wither due to the severe and long-lasting water deficits and VPD, which may hamper the recovery process of ET due to the carryover effect from enhanced forest mortality. The substantial lags of ET recovery and vegetation recovery after the meteorological drought demise (Figure 9b) may be a reflection of drought-induced enhancement of forest mortality in southern Amazon (Wigneron *et al* 2020).

In northern Amazon, the estimation of ET temporal variability is subject to a larger degree of data uncertainty (Figure 6c). Note that northern Amazon is the wettest sub-region in tropical South America where ET is generally energy-limited. Therefore, mild meteorological droughts (e.g., in 2005, 2007, and 2012) do not cause a clear ET response. For the severe meteorological drought in 2010, MODIS ET shows a positive anomaly during the drought and a negative anomaly after the drought demise, while the other three ET products generally show opposite signals, indicating ET regime differences among the products. During the 2016 extreme

meteorological drought, the ET response followed the increase-then-decrease pattern as ET transitioned from an energy-limited to a water-limited regime in three of the datasets, with the exception of MODIS that produced positive ET anomalies especially during the peak of the drought showing no limitation by water availability.

3.3 Vegetative responses

Nearly half of the Earth's vegetated areas have experienced trends that are inconsistent among vegetation cover, greenness and productivity (Ding *et al* 2020). This is especially the case in broadleaf evergreen forests where vegetation greenness and productivity show opposite trends. In addition to the interannual variability and long-term trend, different vegetation indices may respond differently to the same drought event (Yang *et al* 2018). Consistent with previous findings, the trends in vegetation density and productivity are similar in the semiarid Nordeste region, and the two trends contradict each other in the wet Amazonia region. For example, in southern Amazon, SIF (vegetation productivity) features a decreasing signal during 2007-2018 while NDVI (vegetation density) presents an increasing signal (results not shown). To exclude the complicating effects of the trend so to focus on variability at shorter time scales, our analysis on vegetation response to droughts makes use of detrended data in deriving the monthly standardized anomalies of GPP, NDVI, and SIF (Figure 9).

In Nordeste, similar to ET, vegetation is limited by water availability. It therefore responds to drought in a way remarkably similar to ET (and similar to shallow SM), with rapid responses to soil droughts and little delay in recovery (Figure 9a). Note that the mild meteorological droughts in 2005 and 2010 had little impact on vegetation due to the wet soil condition at the drought onset. At the end of the 2012 and 2016 meteorological droughts, vegetation fully recovered with little delay when the shallow SM is replenished by rainfall, and long before the recovery of the deep SM and GRACE TWS. For the same reason, at the breaks between repeated droughts during 2015-2018, vegetation followed the shallow SM to a full recovery while the negative anomalies of deep SM and TWS persisted.

In both the northern and southern Amazon, vegetation indices tend to increase first and then decrease in response to droughts, despite a certain degree of uncertainties or data-dependency (Figures 9b and 9c). This general pattern reflects the transition of vegetation productivity from being limited by light availability to being limited by water availability, similar

to the ET transition from energy limitation to water limitation. In southern Amazon, for example, vegetation indices increased at the onset and during the early stage of the 2016 meteorological drought due to more solar radiation reaching the ground (Figure 8b) while there was still sufficient moisture in the soil; this increase reached its maximum during the monsoon season despite the lower-than-normal precipitation and SM (Figure 7). After the end of the monsoon, the meteorological drought ultimately dried the soil and triggered water stress on vegetation function and growth. Vegetation didn't fully recover until the next monsoon season, and the recovery of SIF and NDVI lagged the return of normal precipitation by two months (Figure 9b). During the extreme 2015-16 drought, the spatial patterns and temporal evolutions of GPP, NDVI, and SIF anomalies show a clear contrast between a "greening" in the Amazonia and a "browning" in Nordeste, and a "greening" in the early stage of the drought followed by a "browning" later in the southern Amazon (Figure 9). The increase-then-decrease pattern was also observed during other drought events in the southern Amazonia, with the exception of NDVI and SIF during a mild 2012 drought. During some droughts, the GPP and SIF responses diverged from the NDVI response, indicating that greenness may not be an accurate indicator of ecosystem function and productivity in humid regions, as also found in previous studies (Yang et al 2018).

In the northern Amazon, due to sufficient moisture availability, adverse effects on vegetation are only evident during severe or extreme droughts; less severe droughts may enhance vegetation growth due to increased solar radiation. The mild meteorological droughts in 2005 and 2007 did not cause a clear plant response (Figure 9c). For the 2012 meteorological drought, the antecedent condition was anomalously wet, likely causing vegetation growth to be light stressed; drought may have provided the condition for vegetation to recover. For the severe drought in 2010 (Figures 2c and 3c), the antecedent period was already drier than normal, with positive vegetation anomalies; by the time of the severe drought onset in 2010, the moisture depletion had advanced enough to trigger water stress and a decrease of vegetation indices. During the extreme drought of 2016, despite the large magnitude of negative standardized anomalies of SM, the level of soil saturation is still high during most of the drought period (Figure 7). This explains the lack of clear vegetation response to drought over most of the northern Amazon. While the use of standardized SM anomalies facilitates comparison among data from different sources, it may not be a reliable indicator for plant water availability in humid regions (which depends on the background climate, vegetation, and soil parameters). The

approximate soil saturation level in Figures 7e1-e6 provides supplementary information that help understand the vegetation response to the 2016 extreme drought in the humid portion of our study domain.

In summary, vegetation responses to drought depend on antecedent SM, root depth, and meteorological drought severity and duration. Wet antecedent conditions can buffer the ecosystem against mild or even moderate drought. In response to severe drought, vegetation greenness and productivity in the dry, shallow-rooted ecosystems (in Nordeste) decrease upon drought onset and recover swiftly at the drought demise; those in the humid, deep-rooted ecosystems (in the Amazon) increase upon drought onset, decrease later as the severe drought progresses, and may take a long time to recover after the drought demise.

4. Conclusions and discussion

In this paper, based on data from multiple sources, we investigate the ecohydrological effects of meteorological droughts in the past two decades in different regions of the tropical South America, and attempt to understand the possible mechanisms underlying the drought response and recovery of different ecohydrological systems. In all three sub-regions we examined, the drought response and recovery of soil moisture, evapotranspiration, vegetation greenness and productivities are influenced by the timing of drought onset and demise relative to the seasonality of precipitation, leading to event specific behaviors. However, several general patterns emerged, as summarized below.

1) Soil moisture: Due to the carryover effect of antecedent soil moisture, a mild meteorological drought in Nordeste may not lead to any soil drought. When a soil drought does occur, the recovery of depleted soil water storage has a longer delay in deep soil than in shallow soil and a longer delay in Nordeste than in the Amazon. This is well demonstrated during 2012-2018 when the deep soil moisture and terrestrial water storage in Nordeste were continuously below normal during the breaks of recurrent meteorological droughts; in contrast, the soil water storage in the Amazon region can achieve full recovery soon after droughts (even in the 2016 extreme drought) or during the breaks of repeated droughts, with generally short time lags.

- 2) Evapotranspiration: In Nordeste, evapotranspiration is highly sensitive to the shallow soil water availability and decreases upon drought onset, as majority of the region is cropland and grassland, both featuring short roots residing in the shallow soil. In the southern Amazon (and northern Amazon too during extreme cases), evapotranspiration during drought tends to increase first and then decrease, shifting from an energy-limited regime to a water-limited regime. After the demise of meteorological droughts, evapotranspiration recovers rapidly in Nordeste with the replenishment of shallow soil moisture, but takes longer to recover in the southern Amazon (longer than both the shallow and deep soil water storage). This may indicate enhanced forest mortality during droughts.
- 3) Vegetation: Vegetative responses are generally consistent with the evapotranspiration responses. In Nordeste, vegetation responds to drought with a decrease of greenness and productivity following the shallow soil moisture signal, and recovery to normal level is rapid during the breaks of repeated drought events such as those in 2012-2018. In the Amazon region, vegetation indices follow a general increase-then-decrease pattern, signifying a drought-induced transition from a light-limited condition to a water-limited condition. In the southern Amazon, negative vegetation anomalies tend to persist well beyond the end of both the meteorological and soil droughts, indicating drought-induced forest mortality that may take a long time to recover from. In the northern Amazon, vegetation anomalies tend to be positive during most droughts, an indication that vegetation has sufficient access to water but benefit from increased light availability during droughts.

In this study, to identify meteorological droughts, we used the standardized anomalies of monthly precipitation as a drought index, which is almost identical to the 1-month Standardized Precipitation Index (SPI, Erfanian *et al* 2017). We then used the intensity and duration of negative index to define three categories of meteorological droughts. There have been no consistent criteria in the literature on what intensity and duration may constitute a mild, severe, or extreme drought. The criteria we chose pertain to our study domain and serve the purpose of analyzing the ecohydrological consequence of droughts at the seasonal to inter-annual time scales. Specifically, mild droughts are events that last for approximately one season with a

commonly used intensity threshold (-0.5σ) , with fairly limited ecohydrological impact; extreme droughts are events that last longer than one year with a greater drought intensity for part of the duration (-1.0σ) , which therefore have major impact on all aspects of the regional ecohydrological system and socioeconomics. A severe drought is in between a mild and an extreme. While the choice of these specific thresholds is subject to discussion, it did capture the major droughts of the region documented in previous studies (Erfanian *et al* 2017).

The general increase-then-decrease pattern in ET and vegetation found in this study is a reflection of a transition from a light-limited regime to a water-limited regime caused by drought, and has important implications for rainforest vulnerability to drought and climate change. Recent studies have indicated that more solar radiation reaching the ground stimulates leaf flush and leaf expansion in the energy-limited Amazon rainforest during dry seasons (Wu et al 2016, Guan et al 2015, Lopes et al 2016). Similar mechanisms could be at work during drought events. "Greening" has been detected repeatedly in recent Amazon droughts (Saleska et al 2007, Yang et al 2018). However, our results showed that as the drought continues, soil water storage may not sustain the continuously elevated evapotranspiration, and the ultimate depletion of soil moisture causes evapotranspiration and photosynthesis to drop, impeding the vegetation growth and productivity and leading to "browning" in Amazon. Therefore, both "greening" and "browning" could take place in the Amazon forest during droughts, depending on the location, severity and stage of the drought.

At the global scale, despite a large degree of uncertainty, drought is projected to generally increase in frequency and severity in a warmer future (Wang 2005, Sheffield and Wood 2008b, Dai 2013, Naumann *et al* 2018, Xu *et al* 2019). This statement qualitatively holds for South America too. A decrease of rainfall and an increase of consecutive dry days over Nordeste are projected, indicating more frequent and more severe droughts (Marengo and Bernasconi 2015, Duffy et al., 2015, Marengo *et al* 2017). Given the observed long delay in soil water storage recovery and continuous soil drought during recurrent meteorological droughts in Nordeste, the prolonged soil drought during 2012-2018 may become the new norm for this region, possibly leading to land degradation and desertification (Marengo and Bernasconi 2015). For the Amazon region, Duffy *et al* (2015) found based on output from 35 CMIP5 climate models that, by the end of the century, the area affected by mild and severe meteorological droughts would nearly

double and triple respectively. This, together with the observed delay of vegetation recovery from severe drought (e.g., Yang *et al* 2018, Wigneron *et al* 2020a), may suggest a future with more frequent recurrence of forest mortality in the southern Amazon, with strong implications on the likelihood of a forest dieback in the Amazon (Cox *et al* 2004, Malhi *et al* 2009).

Acknowledgments

This work was supported by funding from the National Science Foundation (NSF) under Grant AGS-1659953. Computing resources and data storages were provided by the NCAR Computational and Information Systems Laboratory (UCNN0012).

References 499 500 Badgley G, Fisher J B, Jiménez C, Tu K P and Vinukollu R 2015 On uncertainty in global 501 terrestrial evapotranspiration estimates from choice of input forcing datasets J. 502 *Hydrometeorol.* **16** 1449–55 503 De Boeck H J and Verbeeck H 2011 Drought-associated changes in climate and their relevance 504 for ecosystem experiments and models *Biogeosciences* **8** 1121–30 505 Coelho C A S, Cavalcanti I A F, Costa S M S, Freitas S R, Ito E R, Luz G, Santos A F, Nobre C 506 A, Marengo J A and Pezza A B 2012 Climate diagnostics of three major drought events in 507 the Amazon and illustrations of their seasonal precipitation predictions *Meteorol*. Appl. 19 508 237–55 509 Cox P M, Betts R A, Collins M, Harris P P, Huntingford C and Jones C D 2004 Amazonian forest 510 dieback under climate-carbon cycle projections for the 21st century *Theor. Appl. Climatol.* 511 **78** 137–56 512 Dai A 2011 Drought under global warming: A review Wiley Interdiscip. Rev. Clim. Chang. 2 45— 513 65 514 Dai A 2013 Increasing drought under global warming in observations and models Nat. Clim. 515 *Chang.* **3** 52–8 516 Ding Z, Peng J, Qiu S and Zhao Y 2020 Nearly Half of Global Vegetated Area Experienced 517 Inconsistent Vegetation Growth in Terms of Greenness, Cover, and Productivity Earth's 518 *Futur.* **8** 1–15 519 Duffy PB, Brando P, Asner GP and Field CB 2015 Projections of future meteorological drought 520 and wet periods in the Amazon *Proc. Natl. Acad. Sci.* **112** 13172–7 521 Duveiller G and Cescatti A 2016 Spatially downscaling sun-induced chlorophyll fluorescence 522 leads to an improved temporal correlation with gross primary productivity Remote Sens. 523 Environ. **182** 72–89 524 Erfanian A, Wang G and Fomenko L 2017 Unprecedented drought over tropical South America 525 in 2016: significantly under-predicted by tropical SST Sci. Rep. 7 5811

526	Guan K, Pan M, Li H, Wolf A, Wu J, Medvigy D, Caylor K K, Sheffield J, Wood E F, Malhi Y,
527	Liang M, Kimball J S, Saleska S R, Berry J, Joiner J and Lyapustin A I 2015 Photosynthetic
528	seasonality of global tropical forests constrained by hydroclimate Nat. Geosci. 8 284–9
529	Halwatura D, McIntyre N, Lechner A M and Arnold S 2017 Capability of meteorological drought
530	indices for detecting soil moisture droughts J. Hydrol. Reg. Stud. 12 396-412 Online:
531	https://doi.org/10.1016/j.ejrh.2017.06.001
532	Harris I, Osborn T J, Jones P and Lister D 2020 Version 4 of the CRU TS monthly high-resolution
533	gridded multivariate climate dataset Sci. Data 7 1–18
534	Hashimoto H, Wang W, Takenaka H, Higuchi A, Dungan J L, Li S, Michaelis A R, Myneni R B
535	and Nemani R R 2021 observations support seasonality in greenness of the Amazon
536	evergreen forests Nat. Commun. Online: http://dx.doi.org/10.1038/s41467-021-20994-y
537	Hersbach H, Bell B, Berrisford P, Hirahara S, Horányi A, Muñoz-Sabater J, Nicolas J, Peubey
538	C, Radu R, Schepers D, Simmons A, Soci C, Abdalla S, Abellan X, Balsamo G, Bechtold
539	P, Biavati G, Bidlot J, Bonavita M, De Chiara G, Dahlgren P, Dee D, Diamantakis M,
540	Dragani R, Flemming J, Forbes R, Fuentes M, Geer A, Haimberger L, Healy S, Hogan R J,
541	Hólm E, Janisková M, Keeley S, Laloyaux P, Lopez P, Lupu C, Radnoti G, de Rosnay P,
542	Rozum I, Vamborg F, Villaume S and Thépaut J N 2020 The ERA5 global reanalysis Q. J.
543	R. Meteorol. Soc. 146 1999–2049
544	Huete A R, Didan K, Shimabukuro Y E, Ratana P, Saleska S R, Hutyra L R, Yang W, Nemani R
545	R and Myneni R 2006 Amazon rainforests green-up with sunlight in dry season Geophys.
546	Res. Lett. 33 2–5
547	Huffman G J, Adler R F, Bolvin D T, Gu G, Nelkin E J, Bowman K P, Hong Y, Stocker E F and
548	Wolff D B 2007 The TRMM Multisatellite Precipitation Analysis (TMPA): Quasi-global,
549	multiyear, combined-sensor precipitation estimates at fine scales J. Hydrometeorol. 8 38-
550	55
551	IPCC 2014 Climate Change 2014 Part A: Global and Sectoral Aspects Online:
552	papers2://publication/uuid/B8BF5043-C873-4AFD-97F9-A630782E590D
553	Jiang Y, Wang G, Liu W, Erfanian A, Peng Q and Fu R 2020 Modeled Response of South

554	American Climate to Three Decades of Deforestation <i>J. Clim.</i> 1–52
555	Jiménez-Muñoz J C, Mattar C, Barichivich J, Santamaría-Artigas A, Takahashi K, Malhi Y,
556	Sobrino J A and Van Der Schrier G 2016 Record-breaking warming and extreme drought
557	in the Amazon rainforest during the course of El Niño 2015–2016 Sci. Rep. 6 33130
558	Jimenez J C, Libonati R and Peres L F 2018 Droughts over amazonia in 2005, 2010, and 2015:
559	a cloud cover perspective Front. Earth Sci. 6 227
560	Jung M, Reichstein M, Ciais P, Seneviratne S I, Sheffield J, Goulden M L, Bonan G, Cescatti A,
561	Chen J, De Jeu R, Dolman A J, Eugster W, Gerten D, Gianelle D, Gobron N, Heinke J,
562	Kimball J, Law B E, Montagnani L, Mu Q, Mueller B, Oleson K, Papale D, Richardson A
563	D, Roupsard O, Running S, Tomelleri E, Viovy N, Weber U, Williams C, Wood E, Zaehle
564	S and Zhang K 2010 Recent decline in the global land evapotranspiration trend due to
565	limited moisture supply <i>Nature</i> 467 951–4
566	Katul G G, Palmroth S and Oren R 2009 Leaf stomatal responses to vapour pressure deficit
567	under current and CO2-enriched atmosphere explained by the economics of gas exchange
568	Plant, Cell Environ. 32 968–79
569	Kim Y and Wang G 2007a Impact of initial soil moisture anomalies on subsequent precipitation
570	over North America in the coupled land-atmosphere model CAM3-CLM3 J .
571	Hydrometeorol. 8 513–33
572	Kim Y and Wang G 2007b Impact of vegetation feedback on the response of precipitation to
573	antecedent soil moisture anomalies over North America J. Hydrometeorol. 8 534–50
574	Koster R D, Mahanama S P P, Yamada T J, Balsamo G, Berg A A, Boisserie M, Dirmeyer P A,
575	Doblas-Reyes F J, Drewitt G, Gordon C T, Guo Z, Jeong J H, Lawrence D M, Lee W S, Li
576	Z, Luo L, Malyshev S, Merryfield W J, Seneviratne S I, Stanelle T, Van Den Hurk B J J M,
577	Vitart F and Wood E F 2010 Contribution of land surface initialization to subseasonal
578	forecast skill: First results from a multi-model experiment Geophys. Res. Lett. 37 1-6
579	Koster R D and Suarez M J 2001 Soil moisture memory in climate models J. Hydrometeorol. 2
580	558–70
5 81	Kratz D.P. Stackhouse P.W. Gunta S.K. Wilher A.C. Sawaengnhokhai P. and McGarragh G.R.

582 583	2014 The fast longwave and shortwave flux (FLASHFlux) data product: Single-scanner footprint fluxes <i>J. Appl. Meteorol. Climatol.</i> 53 1059–79
584 585 586	Li W and Fu R 2004 Transition of the large-scale atmospheric and land surface conditions from the dry to the wet season over Amazonia as diagnosed by the ECMWF re-analysis <i>J. Clim.</i> 17 2637–51
587 588	Liu D, Wang G, Mei R, Yu Z and Yu M 2014 Impact of initial soil moisture anomalies on climate mean and extremes over Asia <i>J. Geophys. Res. Atmos.</i> 119 529–45
589 590 591	Lopes A P, Nelson B W, Wu J, Graça P M L de A, Tavares J V, Prohaska N, Martins G A and Saleska S R 2016 Leaf flush drives dry season green-up of the Central Amazon <i>Remote Sens. Environ.</i> 182 90–8 Online: http://dx.doi.org/10.1016/j.rse.2016.05.009
592 593 594	Malhi Y, Aragão L E O C, Galbraith D, Huntingford C, Fisher R, Zelazowski P, Sitch S, McSweeney C and Meir P 2009 Exploring the likelihood and mechanism of a climate-change-induced dieback of the Amazon rainforest <i>Proc. Natl. Acad. Sci.</i> 106 20610–5
595 596	Marengo J A and Bernasconi M 2015 Regional differences in aridity/drought conditions over Northeast Brazil: present state and future projections <i>Clim. Change</i> 129 103–15
597 598	Marengo J A, Torres R R and Alves L M 2017 Drought in Northeast Brazil—past, present, and future <i>Theor. Appl. Climatol.</i> 129 1189–200
599 600 601	Martens B, Gonzalez Miralles D, Lievens H, Van Der Schalie R, De Jeu R A M, Fernández-Prieto D, Beck H E, Dorigo W and Verhoest N 2017 GLEAM v3: Satellite-based land evaporation and root-zone soil moisture <i>Geosci. Model Dev.</i> 10 1903–25
602 603 604	Naumann G, Alfieri L, Wyser K, Mentaschi L, Betts R A, Carrao H, Spinoni J, Vogt J and Feyen L 2018 Global Changes in Drought Conditions Under Different Levels of Warming <i>Geophys. Res. Lett.</i> 45 3285–96
605 606 607	Nepstad D C, de Carvalho C R, Davidson E A, Jipp P H, Lefebvre P A, Negreiros G H, da Silva E D, Stone T A, Trumbore S E and Vieira S 1994 The role of deep roots in the hydrological and carbon cycles of Amazonian forests and pastures <i>Nature</i> 372 666–9
608	Panisset J S, Libonati R, Gouveia C M P, Machado-Silva F, Franca D A, Franca J R A and Peres

609	L F 2018 Contrasting patterns of the extreme drought episodes of 2005, 2010 and 2015 in
610	the Amazon Basin Int. J. Climatol. 38 1096–104
611	Rahman M M, Lu M and Kyi K H 2015 Variability of soil moisture memory for wet and dry
612	basins J. Hydrol. 523 107–18 Online: http://dx.doi.org/10.1016/j.jhydrol.2015.01.033
613	Rodell M, Houser PR, Jambor U, Gottschalck J, Mitchell K, Meng CJ, Arsenault K, Cosgrove
614	B, Radakovich J, Bosilovich M, Entin J K, Walker J P, Lohmann D and Toll D 2004 The
615	Global Land Data Assimilation System Bull. Am. Meteorol. Soc. 85 381–94
616	Rodriguez-Iturb I 2000 Ecohydrology: A hydrologic perspective of climate-soil-vegetation
617	dynamics are outlined here , and possible Equation : Questions nZr • = I (s , t) - E (s , t)
618	- L (s,t), I • Plants under I • Plants with no stress Water Resour. Res. 36 3–9
619	Ruosteenoja K, Markkanen T, Venäläinen A, Räisänen P and Peltola H 2018 Seasonal soil
620	moisture and drought occurrence in Europe in CMIP5 projections for the 21st century Clim.
621	<i>Dyn.</i> 50 1177–92
622	Saleska S R, Didan K, Huete A R and Da Rocha H R 2007 Amazon forests green-up during 2005
623	drought Science (80). 318 612
624	Saleska S R, Wu J, Guan K, Araujo A C, Huete A, Nobre A D and Restrepo-Coupe N 2016 Dry-
625	season greening of Amazon forests Nature 531 E4
626	Samanta A, Ganguly S, Hashimoto H, Devadiga S, Vermote E, Knyazikhin Y, Nemani R R and
627	Myneni R B 2010 Amazon forests did not green-up during the 2005 drought Geophys. Res.
628	<i>Lett.</i> 37 1–5
629	Samanta A, Ganguly S and Myneni R B 2011 MODIS enhanced vegetation index data do not
630	show greening of amazon forests during the 2005 drought New Phytol. 189 11-5
631	Schneider U, Becker A, Finger P, Meyer-Christoffer A, Ziese M and Rudolf B 2014 GPCC's
632	new land surface precipitation climatology based on quality-controlled in situ data and its
633	role in quantifying the global water cycle <i>Theor. Appl. Climatol.</i> 115 15-40
634	Seneviratne S I, Corti T, Davin E L, Hirschi M, Jaeger E B, Lehner I, Orlowsky B and Teuling
635	A J 2010 Investigating soil moisture-climate interactions in a changing climate: A review

636	Earth-Science Rev. 99 125–61 Online: http://dx.doi.org/10.1016/j.earscirev.2010.02.004
637	Sheffield J and Wood E F 2008a Global trends and variability in soil moisture and drought
638	characteristics, 1950-2000, from observation-driven simulations of the terrestrial
539	hydrologic cycle J. Clim. 21 432–58
640	Sheffield J and Wood E F 2008b Projected changes in drought occurrence under future global
541	warming from multi-model, multi-scenario, IPCC AR4 simulations Clim. Dyn. 31 79–105
542	Sheffield J, Wood E F and Roderick M L 2012 Little change in global drought over the past 60
543	years <i>Nature</i> 491 435
544	Smith A B and Matthews J L 2015 Quantifying uncertainty and variable sensitivity within the
545	US billion-dollar weather and climate disaster cost estimates Nat. Hazards 77 1829-51
646	Online: http://dx.doi.org/10.1007/s11069-015-1678-x
647	Sörensson A A and Ruscica R C 2018 Intercomparison and Uncertainty Assessment of Nine
548	Evapotranspiration Estimates Over South America Water Resour. Res. 54 2891–908
549	Stocker B D, Zscheischler J, Keenan T F, Prentice I C, Seneviratne S I and Peñuelas J 2019
650	Drought impacts on terrestrial primary production underestimated by satellite monitoring
651	Nat. Geosci. 12 264–70
652	Su B, Huang J, Fischer T, Wang Y, Kundzewicz Z W, Zhai J, Sun H, Wang A, Zeng X and Wang
653	G 2018 Drought losses in China might double between the 1.5° C and 2.0° C warming <i>Proc</i> .
654	Natl. Acad. Sci. 115 10600–5
655	Trenberth K E, Dai A, Van Der Schrier G, Jones P D, Barichivich J, Briffa K R and Sheffield J
656	2014 Global warming and changes in drought Nat. Clim. Chang. 4 17–22
657	United States Department of Agriculture and Service N R C 2005 Chapter 3 Crops Irrig. Guid.
658	NJ3-1-NJ3-7
659	Wang G 2005 Agricultural drought in a future climate: Results from 15 global climate models
660	participating in the IPCC 4th assessment Clim. Dyn. 25 739–53
661	Wang G, Kim Y and Wang D 2007 Quantifying the strength of soil moisture-precipitation
562	coupling and its sensitivity to changes in surface water budget J. Hydrometeorol. 8 551-70

663664	Wang K and Dickinson R E 2012 A review of global terrestrial evapotranspiration: Observation, modeling, climatology, and climatic variability <i>Rev. Geophys.</i> 50
665	Wigneron J-P, Fan L, Ciais P, Bastos A, Brandt M, Chave J, Saatchi S, Baccini A and Fensholt
666	R 2020 Tropical forests did not recover from the strong 2015–2016 El Niño event Sci. Adv.
667	6 eaay4603
668	Wu J, Albert L P, Lopes A P, Restrepo-Coupe N, Hayek M, Wiedemann K T, Guan K, Stark S C,
669	Christoffersen B, Prohaska N, Tavares J V., Marostica S, Kobayashi H, Ferreira M L,
670	Campos K S, Dda Silva R, Brando P M, Dye D G, Huxman T E, Huete A R, Nelson B W
671	and Saleska S R 2016 Leaf development and demography explain photosynthetic
672	seasonality in Amazon evergreen forests Science (80). 351 972-6
673	Wu J, Lakshmi V, Wang D, Lin P, Pan M, Cai X, Wood E F and Zeng Z 2020 The reliability of
674	global remote sensing evapotranspiration products over Amazon Remote Sens. 12
675	Xu L, Chen N and Zhang X 2019 Global drought trends under 1.5 and 2 °C warming Int. J.
676	Climatol. 39 2375–85
677	Xu L, Samanta A, Costa M H, Ganguly S, Nemani R R and Myneni R B 2011 Widespread
678	decline in greenness of Amazonian vegetation due to the 2010 drought Geophys. Res. Lett.
679	38 2–5
680	Yang J, Tian H, Pan S, Chen G, Zhang B and Dangal S 2018 Amazon drought and forest response
681	Largely reduced forest photosynthesis but slightly increased canopy greenness during the
682	extreme drought of 2015/2016 <i>Glob. Chang. Biol.</i> 24 1919–34
683	Yi S, Wang Q and Sun W 2016 Journal of Geophysical Research: Solid Earth J. Geophys. Res.
684	Solid Earth 3782–803
685	Zeng N, Yoon J H, Marengo J A, Subramaniam A, Nobre C A, Mariotti A and Neelin J D 2008
686	Causes and impacts of the 2005 Amazon drought Environ. Res. Lett. 3
687	Zeng X 2001 Global vegetation root distribution for land modeling J. Hydrometeorol. 2 525–30
688	Zhou S, Park Williams A, Berg A M, Cook B I, Zhang Y, Hagemann S, Lorenz R, Seneviratne S
689	I and Gentine P 2019 Land-atmosphere feedbacks exacerbate concurrent soil drought and

690	atmospheric aridity Proc. Na	tl. Acad. Sci. U. S. A.	116 18848–53

693	Table Captions
694	
695	Table 1. Data used in this study.
696	
697	Table 2. Intensity and duration of meteorological droughts.
698	
699	

Table 1. Data used in this study.

Dataset	Туре	Variables	Resolution	Frequency	Record length	References or Dataset DOI
ERA5-Land	Reanalysis	Precipitation, Temperature, Soil Moisture, ET	0.1° x 0.1°	Monthly	1981-Present	(Hersbach et al 2020)
TRMM-3B43	Satellite	Precipitation	0.25° x 0.25°	Monthly	1998-Present	(Huffman et al 2007)
GPCC-V6	Gauge-based	Precipitation	1° x 1°	Monthly	1982-2019	(Schneider et al 2014)
CRU-TS4	Gauge-based	Precipitation, Temperature	0.5° x 0.5°	Monthly	1901-2018	(Harris et al 2020)
GLDAS- NOAH-2.1	Model Simulation	Soil Moisture, ET	0.25° x 0.25°	Monthly	2000-Present	(Rodell et al 2004)
GRACE-JPL	Satellite	Terrestrial Water Storage	0.5° x 0.5°	Monthly	2002-Present	(Yi et al 2016)
MOD16A2GF	Satellite	ET	500m x 500m	8-day	2000-Present	10.5067/MODIS/MOD16A2GF.006
GLEAM-v3.3	Model Simulation	ET	0.25° x 0.25°	Monthly	1980-2018	(Martens et al 2017)
MOD17A2HGF	Satellite	GPP	500m x 500m	8-day	2000-Present	10.5067/MODIS/MOD17A2HGF.006
MOD13C1	Satellite	NDVI	0.05° x 0.05°	16-day	2000-Present	10.5067/MODIS/MOD13C1.006
GOME-2	Satellite	SIF	0.05° x 0.05°	8-day	2007-2018	(Duveiller and Cescatti 2016)
FLASHFlux	Satellite	Solar insolation	0.25° x 0.25°	Monthly	2007-2018	(Kratz et al 2014)

 Table 2. Intensity and duration of meteorological droughts.

	Nordeste	Southern Amazon	Northern Amazon
Mild Drought	September 2004-December 2004	February 2007-September 2007	November 2004-January 2005
	December 2009-March 2010	July 2012-January 2013	January 2007-March 2007
	November 2016-May 2017	June 2017-October 2017	April 2012-July 2012
	September 2017-December 2017	April 2018-June 2018	September 2012-December 2012
			November 2017-March 2018
Severe Drought	April 2007-January 2008	December 2004-October 2005	August 2009-April 2010
	January 2012-September 2012	February 2010-November 2010	April 2017- September 2017
	April 2018-September 2018		
Extreme Drought	August 2015-September 2016	August 2015-July 2016	December 2014-August 2016

707 708 Figure 1. (a-c) Vegetation distribution in 2000 from MODIS, presented as the fractional coverage 709 (%) of different plant types: Trees, Grass and Shrubs, and Crops; (d) annual average precipitation 710 climatology (in mm/day) during 2001-2018 from TRMM; (e) mean seasonal cycle of precipitation 711 (in mm/day) averaged over three sub-regions during 2001-2018, from ERA5, TRMM, GPCC, and 712 CRU. In this study, the tropical South America is divided into three sub-regions: Nordeste (50°W– 713 34°W, 20°S-5°S), southern Amazon (73°W-50°W, 15°S-5°S), and northern Amazon (73°W-714 50°W, 5°S-5°N). 715 716 Figure 2. The three-month moving averages of standardized anomalies of monthly precipitation 717 over a) Nordeste, b) southern Amazon (SouAmazon), and c) northern Amazon (NorAmazon), 718 based on data from ERA5 (black), TRMM (blue), GPCC (red), and CRU (green) during 2001-719 2018. Each year in x-axis starts from January (e.g., 2002 is January 2002). The periods of mild 720 drought, severe drought and extreme drought are highlighted in yellow, orange, and pale red. 721 722 Figure 3. The three-month moving averages of standardized anomalies of monthly soil moisture 723 and terrestrial water storage over a) Nordeste, b) southern Amazon, and c) northern Amazon, 724 based on data for ERA5 shallow soil (0-28cm, green dash line), ERA5 deep soil (100-289cm, 725 green solid line), GLDAS shallow soil (0-40cm, blue dash line), GLDAS deep soil (100-200cm, 726 blue dash line), and GRACE TWS (red solid line) during 2001-2018. The color shading marks 727 the meteorological droughts listed in Table 2. 728 729 Figure 4. Standardized anomalies of deep soil moisture from GLDAS during 2012-2018, relative 730 to the 2001-2018 climatology. 731

706

732

Figure Captions

Figure 5. ET (in mm) variation with shallow soil moisture (a-c, in m³/m³) and VPD (d-f, in mb)

733 in Nordeste (a, d), southern Amazon (b, e), and northern Amazon (c, f). Each data point represents 734 a monthly spatial average over one quarter of each sub-region from ERA5; different seasons are 735 distinguished by color. 736 737 **Figure 6.** The three-month moving averages of standardized anomalies of monthly ET over a) 738 Nordeste, b) southern Amazon, and c) northern Amazon, based on data from ERA5 (black), 739 MODIS (blue), GLEAM (red), and GLDAS (green) during 2001-2018. The color shading marks 740 the meteorological droughts listed in Table 2. 741 742 Figure 7. Standardized anomalies of seasonal shallow soil moisture (a1-a6), NDVI (b1-b6), GPP 743 (c1-c6), and SIF (d1-d6) during the 2016 drought, and the corresponding shallow soil saturation 744 level (e1-e6). Standardized anomalies are relative to statistics during 2007-2018 for SIF and during 745 2001-2018 for all other variables. Soil moisture from GLDAS divided by its 18-year maximum is 746 used as the surrogate for soil saturation in e1-e6. 747 748 Figure 8. The three-month moving averages of the standardized anomalies of monthly CRU near-749 surface temperature (red) during 2001-2018 and FLASHFlux solar insolation (green) during 2007-750 2018, averaged over a) Nordeste, b) southern Amazon, and c) northern Amazon. The color shading 751 marks the meteorological droughts listed in Table 2. 752 753 **Figure 9.** The three-month moving averages of the standardized anomalies of detrended monthly 754 vegetation indices over a) Nordeste, b) southern Amazon, and c) northern Amazon, based on 755 MODIS NDVI (blue) and MODIS GPP (green) during 2001-2018, and GOME2 SIF (red) during

2007-2018. The color shading marks the meteorological droughts listed in Table 2.

756

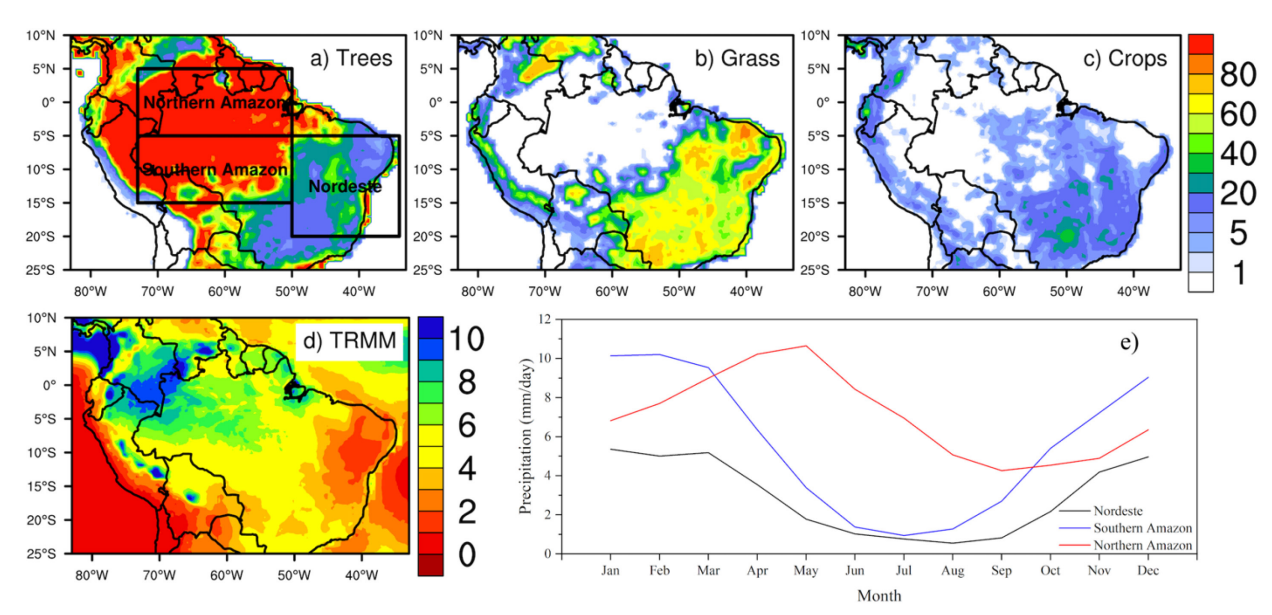


Figure 1. Vegetation distribution in 2000 from MODIS, in the fractional coverage (%) of different plant types: Trees (a), Grass (b), and Crops (c); annual average precipitation climatology (d; mm/day) from TRMM during 2001-2018; monthly average precipitation (e; mm/day) over three sub-regions, averaged from ERA5, TRMM, GPCC, and CRU during 2001-2018. In this study, the tropical South America is divided into three sub-regions: Nordeste (50°W–34°W, 20°S–5°S), southern Amazon (73°W–50°W, 15°S–5°S), and northern Amazon (73°W–50°W, 5°S–5°N).

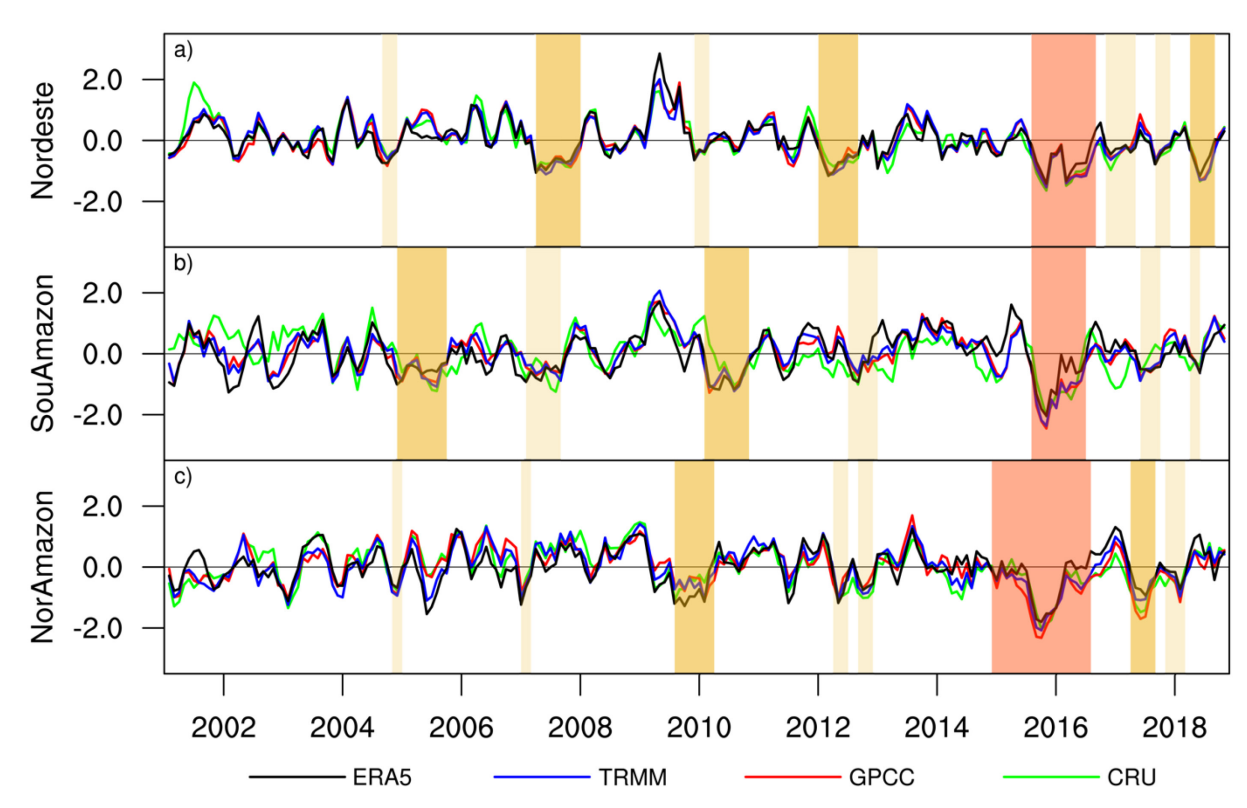


Figure 2. The three-month moving averages of standardized anomalies of monthly precipitation over a) Nordeste, b) southern Amazon (SouAmazon), and c) northern Amazon (NorAmazon) from ERA5 (black), TRMM (blue), GPCC (red), and CRU (green) during 2001-2018. Each year in x-axis starts from January (e.g., 2002 is January 2002). The periods of mild drought, severe drought and extreme drought have been highlighted in yellow, orange, and pale red.

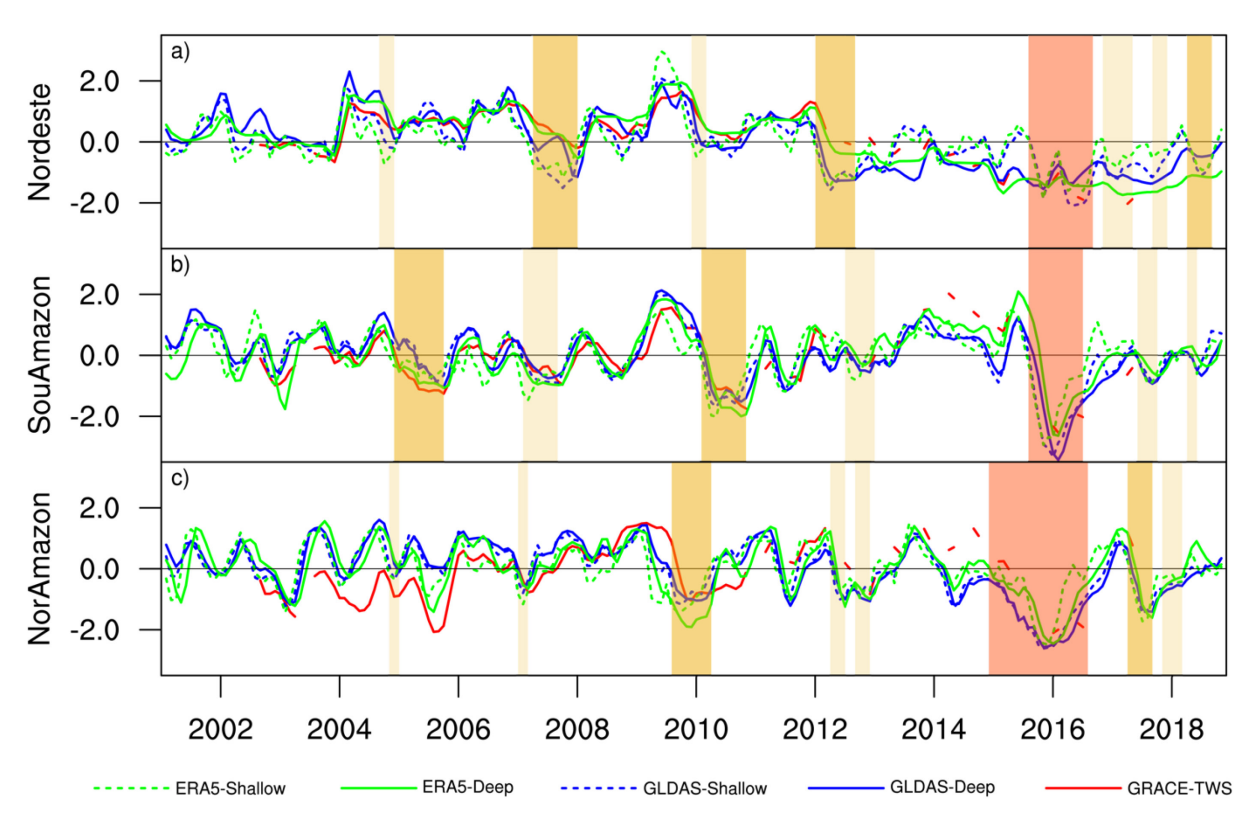


Figure 3. The three-month moving averages of standardized anomalies of monthly soil moisture and terrestrial water storage over a) Nordeste, b) southern Amazon, and c) northern Amazon from ERA5 shallow soil (0-28cm, green dash line), ERA5 deep soil (100-289cm, green solid line), GLDAS shallow soil (0-40cm, blue dash line), GLDAS deep soil (100-200cm, blue dash line), and GRACE TWS (red solid line) during 2001-2018. The color shading marks the meteorological droughts listed in Table 2.

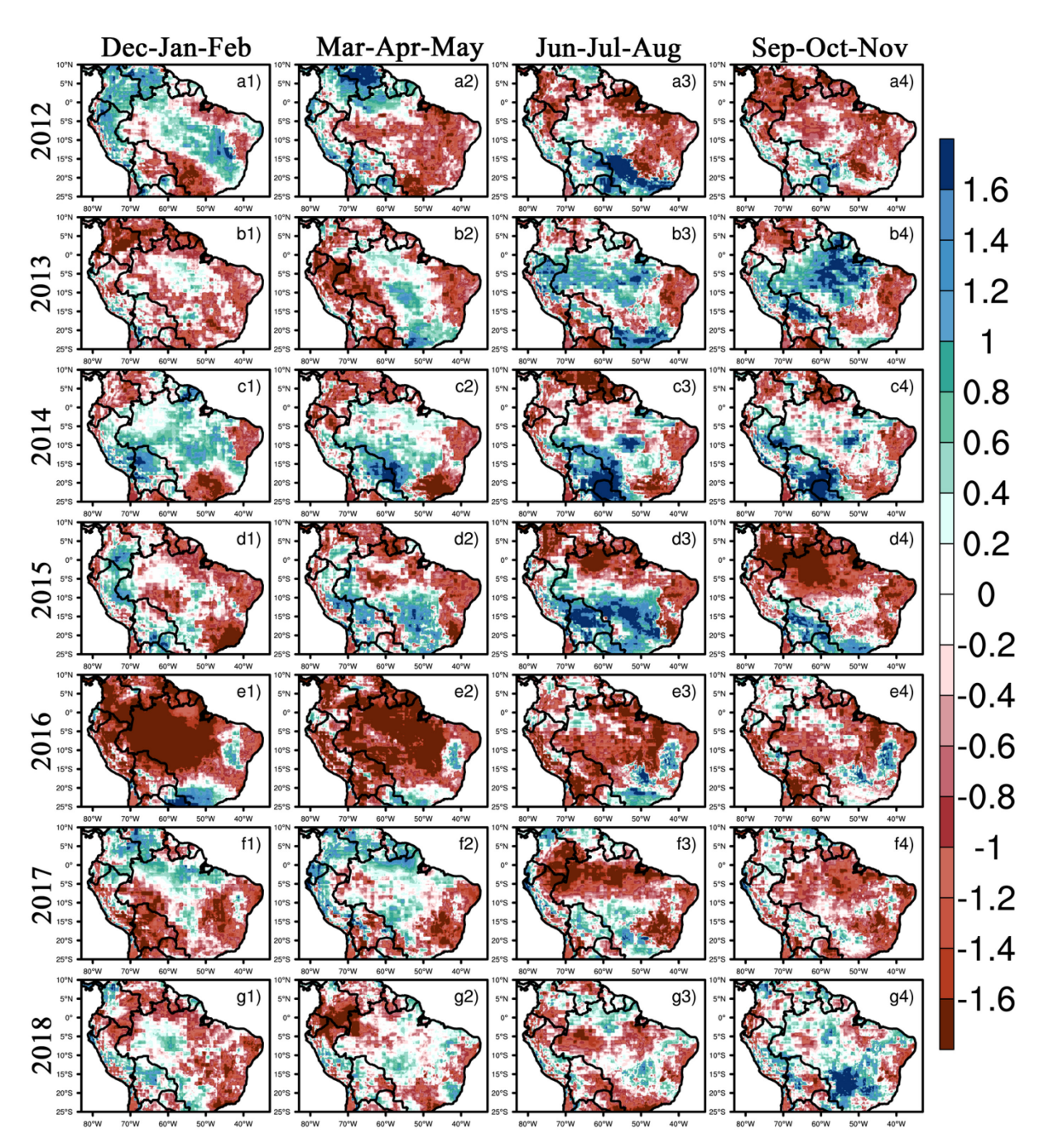


Figure 4. Standardized anomalies of deep soil moisture from GLDAS during 2012-2018, relative to climatology over 2001-2018.

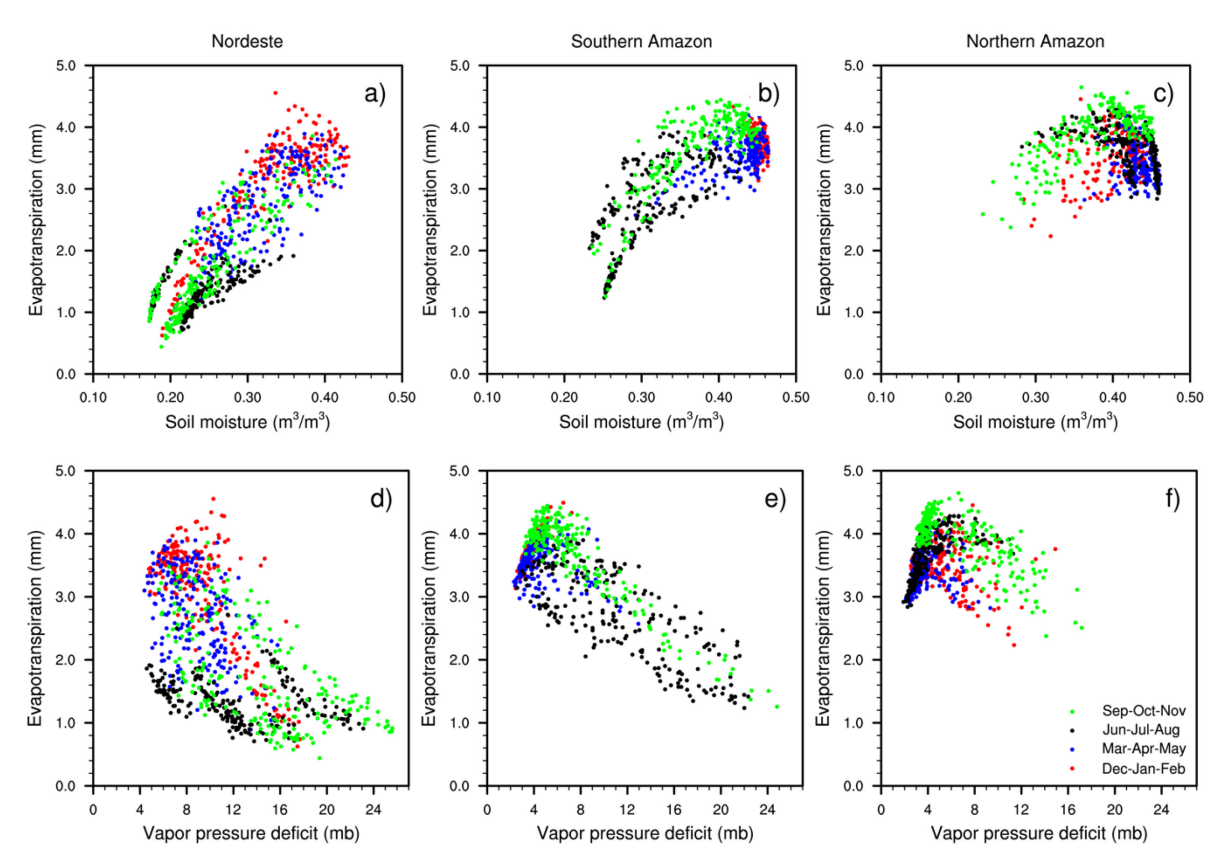


Figure 5. ET (mm) variation with shallow soil moisture (a-c; m³/m³) and VPD (d-f; mb) in Nordeste (a, d), southern Amazon (b, e), and northern Amazon (c, f). Each data point represents a monthly spatial average over one quarter of each sub-region from ERA5; different seasons are distinguished by color.

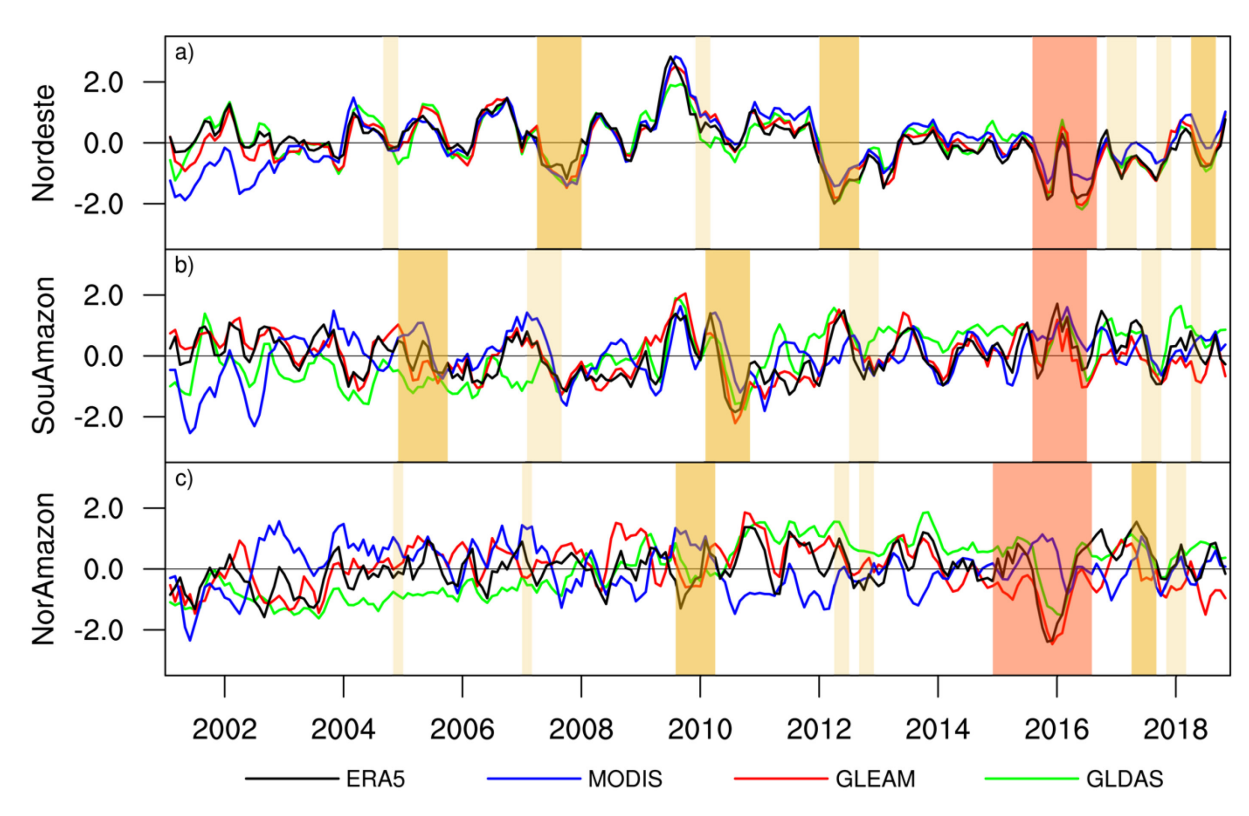


Figure 6. The three-month moving averages of standardized anomalies of monthly ET over a) Nordeste, b) southern Amazon, and c) northern Amazon from ERA5 (black), MODIS (blue), GLEAM (red), and GLDAS (green) during 2001-2018. The color shading marks the meteorological droughts listed in Table 2.

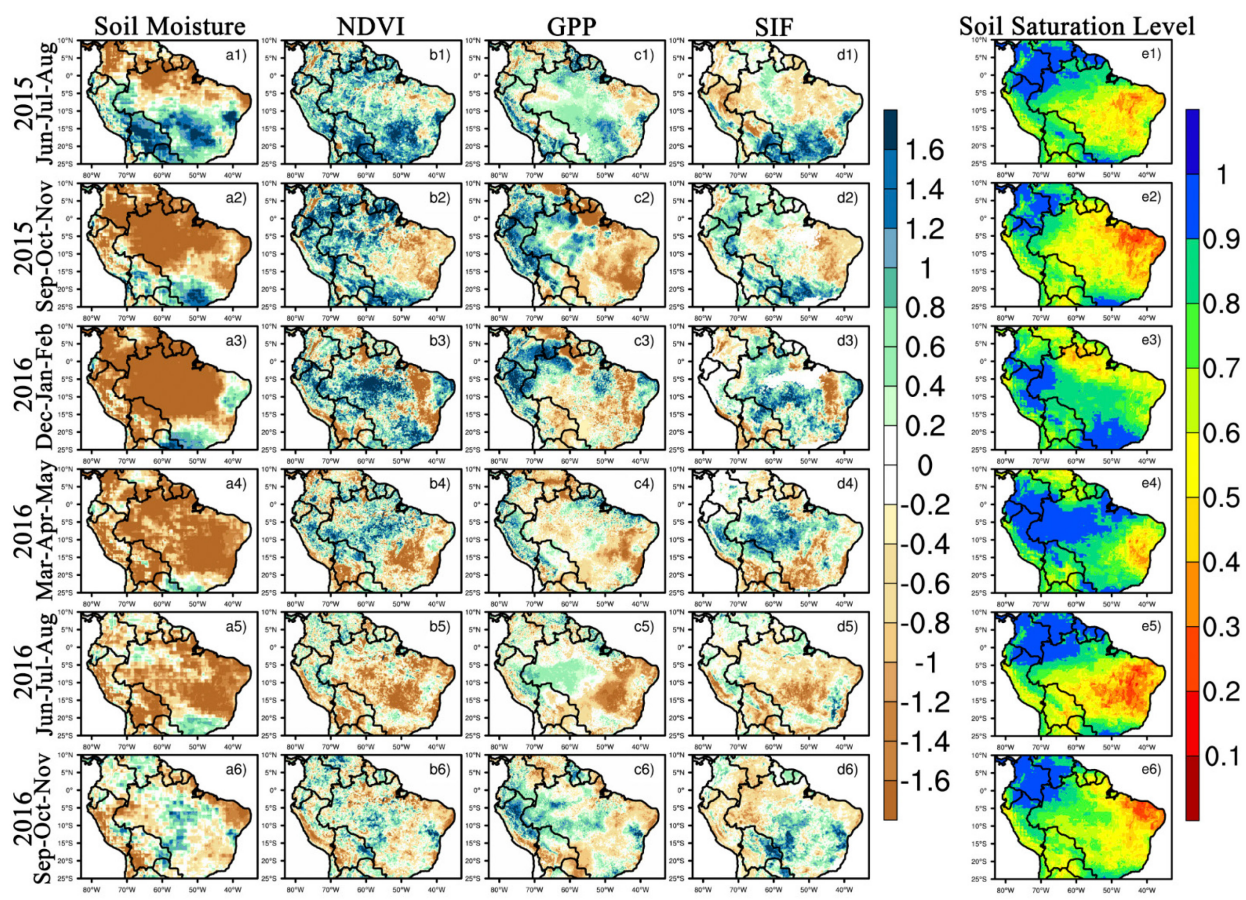


Figure 7. Standardized anomalies of seasonal shallow soil moisture (a1-a6), NDVI (b1-b6), GPP (c1-c6), and SIF (d1-d6), and the corresponding shallow soil saturation level (e1-e6) during the 2016 drought. Standardized anomalies are relative to statistics during 2007-2018 for SIF and 2001-2018 for all other variables. Soil moisture from GLDAS divided by its 18-year maximum was used as the surrogate for soil saturation in e1-e6.

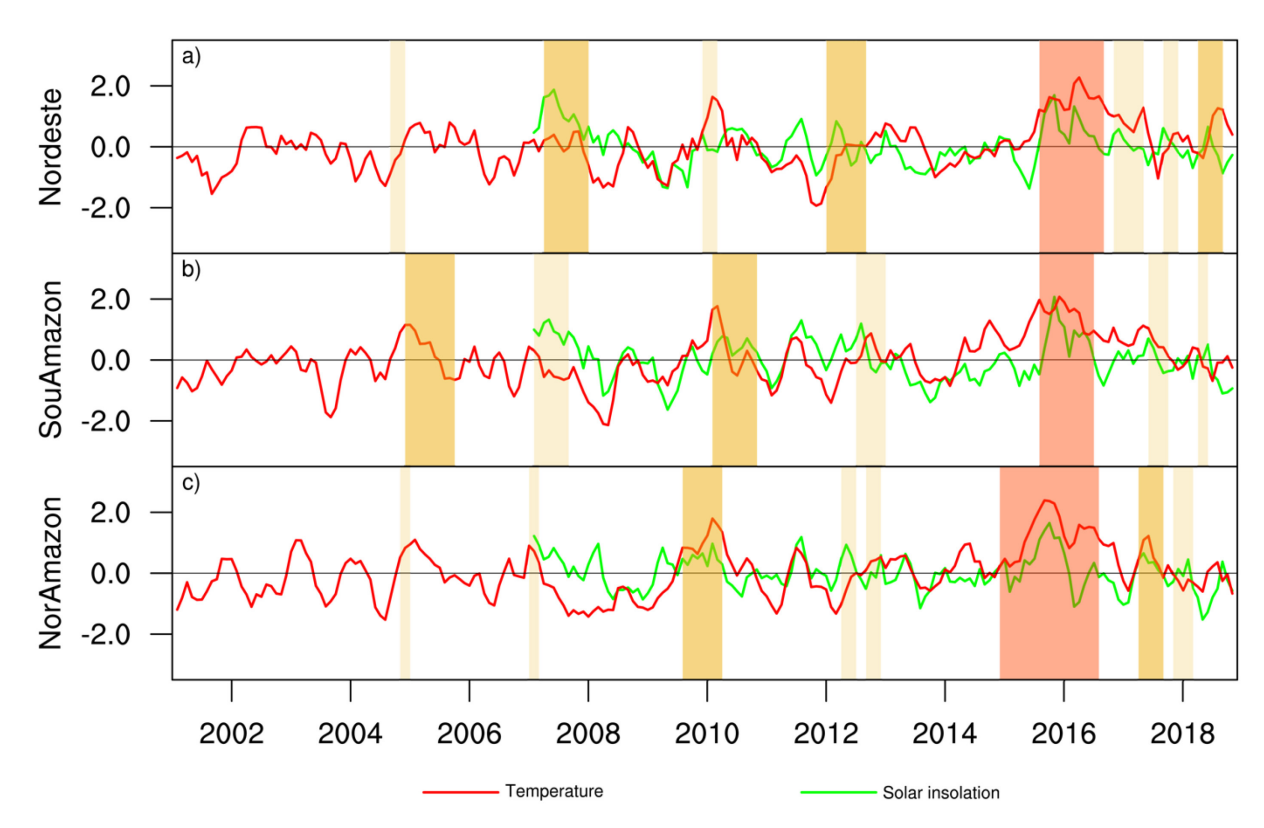


Figure 8. The three-month moving averages of the standardized anomalies of monthly CRU near-surface temperature (red) during 2001-2018 and FLASHFlux solar insolation (green) during 2007-2018 over a) Nordeste, b) southern Amazon, and c) northern Amazon from data. The color shading marks the meteorological droughts listed in Table 2.

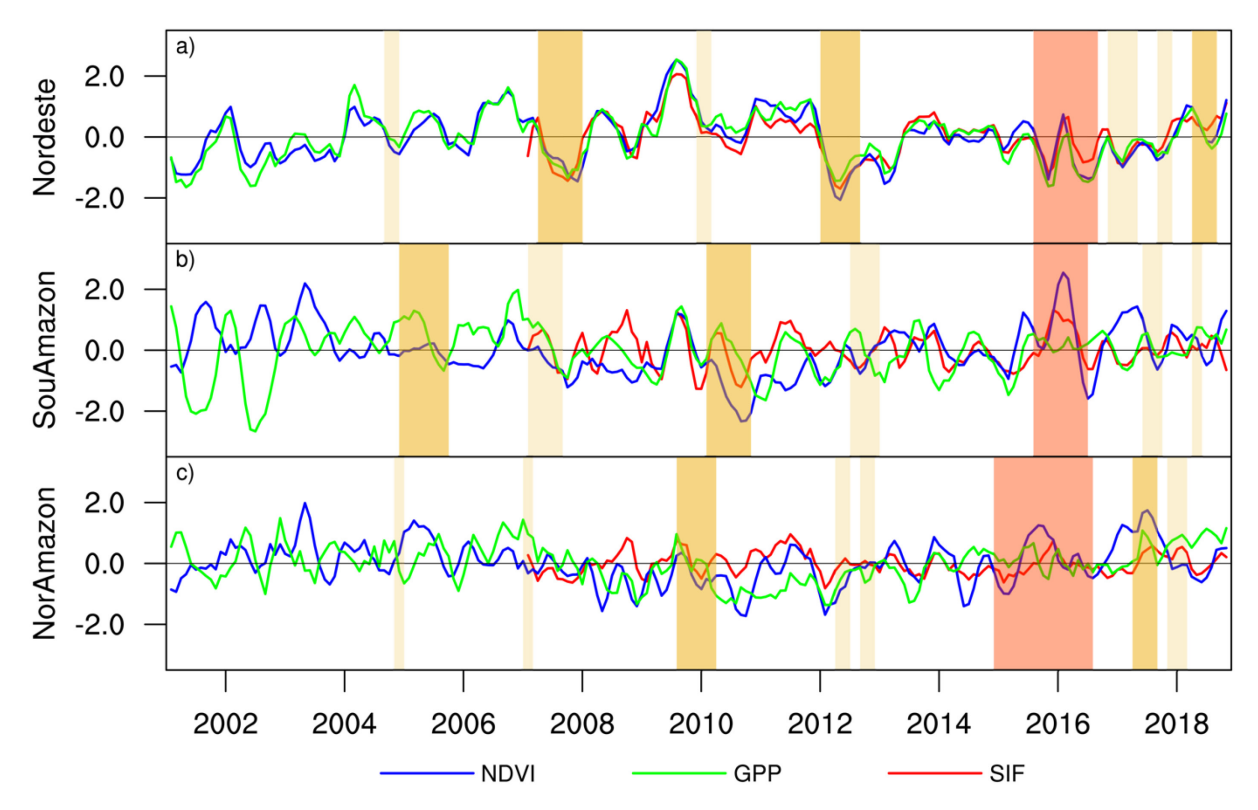


Figure 9. The three-month moving averages of the standardized anomalies of detrended monthly vegetation indices over a) Nordeste, b) southern Amazon, and c) northern Amazon from MODIS NDVI (blue) and MODIS GPP (green) during 2001-2018, and GOME2 SIF (red) during 2007-2018. The color shading marks the meteorological droughts listed in Table 2.